Self-regulating genomic island encoding tandem regulators confers chromatic acclimation to marine Synechococcus

Joseph E. Sanfilippo, Adam A. Nguyen, Jonathan A. Karty, Animesh Shukla, Wendy M. Schluchter, Laurence Garczarek, Frédéric Partensky, David M. Kehoe

Self-regulating genomic island encoding tandem regulators confers chromatic acclimation to marine *Synechococcus*

Joseph E. Sanfilippo[a], Adam A. Nguyen[b,c], Jonathan A. Karty[d], Animesh Shukla[a], Wendy M. Schluchter[b,c], Laurence Garczarek[e], Frédéric Partensky[e], and David M. Kehoe[a,f]

[a]Department of Biology, Indiana University, Bloomington, IN 47405; [b]Department of Biological Sciences, University of New Orleans, New Orleans, LA 70148; [c]Department of Chemistry, University of New Orleans, New Orleans, LA 70148; [d]Mass Spectrometry Facility, Department of Chemistry, Indiana University, Bloomington, IN 47405; [e]Sorbonne Universités, Université Pierre et Marie Curie University Paris 06, CNRS, UMR 7144, Station Biologique, Plankton Group, 29688 Roscoff, France; and [f]Indiana Molecular Biology Institute, Indiana University, Bloomington, IN 47405

Edited by Elisabeth Gantt, University of Maryland, College Park, MD, and approved March 31, 2016 (received for review January 13, 2016)

This article is a PNAS Direct Submission.

Author contributions: J.E.S., J.A.K., A.S., W.M.S., and D.M.K. designed research; J.E.S., A.A.N., J.A.K., A.S., and W.M.S. performed research; J.E.S., A.A.N., J.A.K., A.S., W.M.S., L.G., F.P., and D.M.K. analyzed data; and J.E.S., A.A.N., J.A.K., W.M.S., L.G., F.P., and D.M.K. wrote the paper.

The authors declare no conflict of interest.

Key words: horizontal gene transfer | phycobilisome | marine cyanobacteria | marine biology | light regulation

Abstract

The evolutionary success of marine *Synechococcus*, the second most abundant phototrophic group in the marine environment, is partly attributable to this group's ability to use the entire visible spectrum of light for photosynthesis. This group possesses a remarkable diversity of light-harvesting pigments, and most of the group's members are orange and pink because of their use of phycourobilin and phycoerythrobilin chromophores, which are attached to antennae proteins called phycoerythrins. Many strains can alter phycoerythrin chromophore ratios to optimize photon capture in changing blue–green environments using type IV chromatic acclimation (CA4). Although CA4 is common in most marine *Synechococcus* lineages, the regulation of this process remains unexplored. Here, we show that a widely distributed genomic island encoding tandem master regulators named FciA (for type four chromatic acclimation island) and FciB plays a central role in controlling CA4. FciA and FciB have diametric effects on CA4. Interruption of *fciA* causes a constitutive green light phenotype, and interruption of *fciB* causes a constitutive blue light phenotype. These proteins regulate all of the molecular responses occurring during CA4, and the proteins' activity is apparently regulated posttranscriptionally, although their cellular ratio appears to be critical for establishing the set point for the blue–green switch in ecologically relevant light environments. Surprisingly, FciA and FciB coregulate only three genes within the *Synechococcus* genome, all located within the same genomic island as *fciA* and *fciB*. These findings, along with the widespread distribution of strains possessing this island, suggest that horizontal transfer of a small, self-regulating DNA region has conferred CA4 capability to marine *Synechococcus* throughout many oceanic areas.

Significance

The regulation of photosynthesis in marine phytoplankton, which account for approximately half the Earth's primary productivity, is fundamentally important but not well understood. Picocyanobacteria such as *Synechococcus*, which are responsible for 10–20% of global marine productivity, live in environments where light availability often limits photosynthesis. CA4 is a process commonly used by *Synechococcus* to optimize photon capture under such conditions. We characterize CA4 regulation by demonstrating that two proteins, FciA and FciB (for type four chromatic acclimation island), operate diametrically to control CA4 in response to changes in the ratio of blue to green light. The genes encoding these proteins, and the genes they both regulate, are contained within a widespread genomic island that is likely sufficient for horizontal transfer and expansion of this phenotype.

Introduction

Cyanobacteria of the genus *Synechococcus* are broadly distributed in the marine environment and with an estimated global cell population of 7 × 1026 cells, constitute the second most abundant group of phytoplankton on Earth (1). The ubiquitous distribution of *Synechococcus* spp. is attributable in part to the group's capacity to effectively use the diverse light colors available in the aquatic environment for photosynthesis (2). *Synechococcus* contain hemi-discoidal photosynthetic light-harvesting antennae, known as phycobilisomes, comprising multiple rods extending from a central core. Every rod consists of a stack of disk-shaped structures, with each disk containing six heterodimers of α and β phycobiliprotein subunits (3). There are many types of phycobiliproteins, each possessing a unique set of bilin chromophores for light capture. Chromophores are covalently attached to one or more specific cysteine residues within each phycobiliprotein either by a lyase or a lyase/ isomerase (4, 5). The rods of marine *Synechococcus* always contain α and β subunits of the phycobiliprotein phycocyanin (PC) and usually also have one or two forms of phycoerythrin (PE), phycoerythrin I (PEI), and phycoerythrin II (PEII) (2, 3). In addition to using the red-absorbing chromophore phycocyanobilin [absorbance maximum (λmax) ∼660 nm], many *Synechococcus* strains have adapted to blue-/green-rich waters by incorporating the blue light-absorbing chromophore phycourobilin (PUB) (λmax ∼495 nm) and/ or the green light-absorbing chromophore phycoerythrobilin (PEB) (λmax ∼550 nm) into their phycobilisomes (6).

Some marine *Synechococcus* strains are blue light specialists (high PUB content) or green light specialists (high PEB content), whereas other strains are capable of changing the PUB:PEB ratio within their phycobilisomes in response to changes in the ambient blue:green light ratio through a process known as type IV chromatic acclimation (hereafter called CA4) (2, 7–9). *Synechococcus* capable of CA4 increase the amount of PUB per phycobilisome in blue light and increase the amount of PEB per phycobilisome in green light. CA4 and related chromatic acclimation responses are useful low-light acclimation processes, optimizing photon capture and photosynthetic activity, perhaps most importantly when irradiance levels limit photosynthesis (10–13). Chromatic acclimation provides a fitness advantage and allows niche exploitation in freshwater and marine environments, where water depth and seasonal fluctuations change the ambient spectral distribution (14, 15). CA4 occurs in approximately one-fourth of all marine *Synechococcus* strains sequenced to date from most lineages and is therefore likely to be a globally important process (16). Despite its importance, mechanistic insights into CA4 are limited, and nothing is known about its regulation. However, a 5-kb genomic island has been identified whose presence correlates with the CA4 capability of *Synechococcus* strains isolated from various locations around the world (2, 16). Although marine *Synechococcus* strains have been shown to horizontally acquire genomic islands that confer novel traits other than CA4, such as antibiotic production (17) or stress tolerance (18), how *Synechococcus* genomic island gene expression is regulated remains unknown.

Using *Synechococcus* sp. RS9916 (hereafter 9916) as a CA4 model organism, we discovered that CA4-mediated chromophorylation changes occur at cysteines 83 (C83) and C140 within α-PEII (MpeA) and C139 within α-PEI (CpeA) (9). We also identified, within the CA4 genomic island, a gene encoding a lyase/ isomerase called MpeZ that contributes to the CA4 response by attaching PUB to C83 within MpeA in blue light. The levels of *mpeZ* transcripts were found to be higher in blue light than green light, but how this is regulated remains unclear. Also, the enzyme(s) that control the CA4-mediated chromophorylation of MpeA-C140 and CpeA-C139 have not been identified.

Here, we demonstrate that two additional proteins encoded within the CA4 genomic island, FciA (for type four chromatic acclimation island) and FciB, are master regulators of this process. We show

that, despite being encoded by the same operon, FciA and FciB have diametric effects during CA4 and synergistically control all differential chromophorylation in blue and green light. We demonstrate that although FciA and FciB are the essential regulators of CA4, collectively they regulate only three genes, all of which are also located within the CA4 genomic island. Taken together, our results suggest that horizontal gene transfer of this small, self-regulating genomic island confers CA4 to marine *Synechococcus* in specific ecological niches throughout the world's oceans.

Results

FciA and FciB Are Master Regulators of CA4. The presence of a small genomic island in all CA4-capable strains of *Synechococcus* and the dispersed nature of CA4 throughout the *Synechococcus* radiation suggests that horizontal gene transfer has played a large role in the expansion of CA4 throughout this group (2, 7, 16, 19). Additional support for this hypothesis is provided by the 44% GC content of the DNA that comprises the CA4 genomic island in 9916, which is markedly different from the 61% GC content of the regions bordering the island (Fig. 1A) and the 60% GC content of the entire genome (16). The island is also flanked by one complete copy and one fragment of the psbA gene, which is a proposed hotspot for DNA-recombination events (16, 20). We hypothesized that two proteins encoded within the CA4 genomic island, FciA and FciB, are CA4 regulators because both are putative AraC-class transcription factors and every sequenced CA4 strain contains *fciA* and *fciB* within its CA4 genomic island (16, 21). In 9916, the coding regions of *fciA* and *fciB* overlap by a single base pair. These genes are apparently cotranscribed (Fig. S1 A and B), and their transcript levels are similar in blue and green light (Fig. S1 C and D).

Insertion mutants of *fciA* and *fciB* were created (Fig. S2) and tested for their ability to carry out CA4, which turns WT 9916 cells pink in green light and orange in blue light because of shifts in the PUB:PEB ratio within the phycobilisomes. However, *fciA* mutant cells always appear pink, and *fciB* mutant cells always appear orange (Fig. 1B). The ability of each mutant to carry out CA4 was examined by measuring the 495 nm:545 nm fluorescence excitation ratio with emission set at 580 nm (hereafter Ex495:545 ratio), which serves as a proxy for their in vivo PUB:PEB ratio (8, 9). Cells grown in green light were switched to blue light, then returned to green light, over a 28-d period. Whereas control cells harboring a CA4-neutral insertion underwent normal acclimation to blue light and re-acclimation to green light over 5–6 d, the Ex495:545 ratios for the *fciA* and *fciB* mutant cells remained unchanged during the 28-d experiment (Fig. 1C). However, the phenotypes of the two mutants were completely opposite, with *fciA* mutant cells locked in the green light state and *fciB* mutant cells locked in the blue light state. Therefore, the two genomic island-encoded genes *fciA* and *fciB* are both necessary for cells to carry out CA4.

The possibility that these phenotypes were attributable to polar effects was tested by introducing WT versions of either *fciA*, *fciB*, or both genes in tandem into each mutant using an autonomously replicating plasmid and measuring Ex495:545 ratios for transformants that were fully acclimated to either blue or green light (Fig. 1D). There is no polar effect of the *fciA* interruption on *fciB* because the mutant phenotype was complemented when *fciA* alone was reintroduced. Although fciB did not complement the *fciA* mutant, *fciA* and *fciB* together did. In contrast, the fciB mutation was complemented by *fciA* and *fciB* together but was not complemented by either *fciB* or *fciA* alone. Although introducing *fciA* had no effect on the *fciB* mutant, the introduction of fciB decreased the Ex495:545 ratio of the *fciB* mutant to a value similar to that of the *fciA* mutant, in both light colors. One possible explanation for this phenotype is that *fciB* is being expressed above WT levels from the

plasmid, thus altering the CA4 response. We tested this possibility by transforming WT cells with the plasmids used for complementation and measuring *fciA* and *fciB* RNA levels after growth in blue and green light. *fciA* and *fciB* were expressed approximately 5to 10-fold higher in these transformants than in WT cells containing an empty vector (Fig. S1 E–H). Overexpression of *fciA* increased the Ex495:545 ratio in green light, similar to the *fciB* mutant phenotype, whereas *fciB* overexpression decreased the Ex495:545 ratio in blue light, similar to the *fciA* mutant phenotype (Fig. 1D). Overexpressing fciA and *fciB* together did not affect the Ex495:545 ratio, suggesting that the FciA:FciB ratio is critical for normal CA4. In summary, overexpression of either *fciA* or *fciB* individually, but not together, is sufficient to disrupt CA4.

The parameters of the CA4 response that are regulated by FciA and FciB were initially examined by purifying phycobilisomes from WT, *fciA* mutant, and *fciB* mutant cells fully acclimated to blue or green light. Individual components were separated by HPLC, each phycoerythrin subunit was individually isolated, and UV–visible (UV-VIS) absorption spectroscopy used to determine chromophore composition (Fig. 2). During CA4 in 9916, differential chromophorylation occurs at three positions: MpeA-C83, MpeA-C140, and CpeA-C139. All three bind PUB in blue light and PEB in green light. Two positions in these α subunits are not affected by CA4: MpeA-C75 binds PUB and CpeA-C82 binds PEB in both blue and green light (9). The CA4-mediated chromophorylation changes of MpeA and CpeA strongly affect the overall absorbance characteristics of these two proteins (Fig. 2 A and D). The chromophore composition of the phycoerythrin β subunits MpeB (β-PEII) and CpeB (β-PEI) is unchanged by CA4 (Fig. S3) (9).

Purification and spectral analyses of phycobiliprotein subunits from *fciA* and *fciB* mutant cells grown in blue or green light revealed that both lacked any CA4-mediated chromophorylation changes within either MpeA or CpeA (Figs. 2 B, C, E, and F) or MpeB or CpeB (Fig. S3). The absorbance characteristics of MpeA and CpeA from *fciA* mutant cells grown in blue or green light matched WT cells grown in green light, whereas MpeA and CpeA from *fciB* mutant cells grown in blue or green light matched WT cells grown in blue light. The specific chromophorylation patterns within MpeA and CpeA in these mutants after growth in blue and green light were analyzed by UV-VIS absorption spectroscopy coupled to mass spectrometry. These data confirmed that during growth in blue and green light, *fciA* mutant cells had PEB at positions CpeA-C139, MpeA-C83, and MpeA-C140, whereas *fciB* mutant cells had PUB at these residues (Figs. S4 and S5). Collectively, these data demonstrate that FciA and FciB are master regulators of CA4 that control all differential chromophorylation that occurs during CA4.

FciA and FciB Inversely Regulate Expression of Several Genomic Island Genes During CA4. Based on the absence of CA4-mediated chromophorylation changes in *fciA* and *fciB* mutants, we hypothesized that FciA and FciB control CA4-regulated gene expression. To identify regulatory targets of FciA and FciB, we conducted RNA sequencing (RNA-Seq) of control, *fciA* mutant, and *fciB* mutant cells grown in blue or green light. Surprisingly, data from control cells grown in either blue or green light revealed that only five genes in the 9916 genome had a statistically significant difference in RNA abundance during CA4 (Table S1). All five genes were more highly expressed in blue light than in green light, and the three genes most strongly regulated by CA4, *mpeZ* (35-fold), *fciC* (10-fold), and *unk10* (40-fold), are located within the same genomic island as *fciA* and *fciB* (Fig. 1A).

Based on the constitutive green light phenotype of the *fciA* mutant and the fact that all five genes were normally more highly expressed in blue light, we predicted that FciA activates gene expression in blue light. Genome-wide transcript levels from control and *fciA* mutant cells grown in blue light were compared to identify genes deactivated in the *fciA* mutant. The results in Table S1 show that FciA is only responsible for the blue light activation of the three most highly CA4-regulated genes,

mpeZ, *fciC*, and *unk10*. The constitutive blue light phenotype of the *fciB* mutant suggested that FciB is a repressor of gene expression in green light. Therefore, global RNA levels from control and *fciB* mutant cells grown in green light were compared to identify genes derepressed in the *fciB* mutant. FciB was responsible for the green light-mediated repression of nine genes, with the three most strongly repressed genes, *mpeZ*, *fciC*, and unk10, also differentially regulated during CA4 and activated by FciA (Table S1). The quantified expression levels of *mpeZ*, *fciC*, and *unk10* in control, *fciA*, and fciB mutant cells clearly indicate that FciA activates and FciB represses expression of *mpeZ*, *fciC*, and *unk10* (Fig. 3 A–C). Independent expression data obtained from RNA blot analyses confirmed the RNA-Seq results (Fig. S6). Taken together, these results demonstrate that *mpeZ*, *fciC*, and *unk10* are the only genes regulated by both FciA and FciB (Fig. 3D), indicating that the CA4 regulon consists exclusively of genes located within the CA4 genomic island.

Relative Expression of fciA and fciB Determines the Blue–Green Light Midpoint for CA4. The diametric control of CA4 by FciA and FciB suggests that their functions are integrated and, thus, responsive to the ratio of blue to green light in their environment rather than the overall amount of either. We measured the Ex495:545 ratios to examine the capacity of 9916 to acclimate to a series of blue–green light ratios that closely mimic its natural environment (Fig. 4) (14). Cells continued to behave as if they were in a pure light color when slight amounts of the other color was also provided, such as at a ratio of 9 μmol green photons m^{-2} s^{-1}:1 μmol blue photons m^{-2} s^{-1} (9G:1B) or at a 1G:9B ratio. The 9916 CA4 response reached the halfway point between the green light- and blue light-acclimated states as determined by the Ex495:545 ratios (CA4 midpoint value; Ex495:545 ~1.1) between ratios of 5G:5B and 4G:6B. Based on this response, we hypothesized that cells were either responding to the ratio of blue to green light or the absolute amount of irradiance of one light color. We found that although both 7G:3B and 3G:7B only slightly triggered CA4 (Fig. 4), providing as little as 3G:0B or 0G:3B was sufficient to elicit a full CA4 response (Fig. S7). Therefore, we conclude that 9916 is capable of regulating CA4 by assessing the ratio, rather than the absolute amounts, of blue and green light in its environment.

In addition, the relative expression of *fciA* and *fciB* affects the CA4 midpoint value in 9916 (Fig. 4). Overexpression of *fciA* sensitized the cells to blue light, so that any light color ratio equal to or below 7G:3B was sensed as pure blue light. Conversely, *fciB* overexpression sensitized cells to green light such that the cells sensed any light color ratio equal to or above 3G:7B as pure green light. These results were attributable to changes in the in vivo *fciA*:*fciB* expression ratio, because the CA4 midpoint value of cells overexpressing both *fciA* and *fciB* was more similar to that of the control cells than cells overexpressing either *fciA* or *fciB* alone (Fig. 4). Together, these results suggest that the effects of FciA and FciB are integrated to establish the CA4 midpoint value for 9916 and raise the possibility that the CA4 response could be influenced by changes in the relative activity or abundance of these proteins. Our RNA-Seq results suggest that for 9916, the CA4 response is unlikely attributable to abundance changes, because neither *fciA* nor *fciB* expression changes during CA4 (Fig. S1 C and D).

Discussion

CA4 is a prevalent process within the marine *Synechococcus* radiation, because 14 of the 40 genomes of isolates sequenced thus far in this group were shown to contain a complete CA4 genomic island containing a *fciAB* operon (16), and strains showing this trait have been isolated from many different sites in the ocean in the vicinity of continents (Fig. 5A). By improving the efficiency of photon capture by *Synechococcus* phycobilisomes, CA4 is likely to significantly influence global primary productivity

in the marine environment. We propose that horizontal acquisition of the CA4 genomic island, which always contains *fciA* and *fciB* (16), is sufficient to impart the ability to perform CA4. Because of the widespread nature of *Synechococcus* and CA4, this evolutionary mechanism is likely critical for niche adaptation to mixed waters and/or transition areas between coastal and offshore waters, as illustrated by the large proportion of CA4-capable cells in the permanently mixed waters of the English Channel (22). Here, we have identified FciA and FciB as two central regulators of CA4 and shown the diametric influence of each of these proteins on genomic island gene expression, differential phycobilisome chromophorylation, and blue– green responsiveness.

Our data are consistent with FciA functioning as an activator in blue light and FciB serving as a repressor in green light of the expression of three genes, all of which are located within the CA4 genomic island (Fig. 5B). We propose that, in mesotrophic and coastal waters, where blue light is more attenuated than green light and PEB is more effective than PUB for light harvesting (23), FciB represses CA4 gene expression, whereas FciA activates CA4 gene expression in open ocean oligotrophic waters, where blue light is transmitted better than green light and PUB is more effective for light harvesting than PEB (23). Together, FciA and FciB tune gene expression levels in response to the ambient blue to green ratio (Fig. 5B). A decrease in this ratio causes repression of gene expression by FciB to overcome activation by FciA, leading to low expression of *mpeZ*, *fciC*, and *unk10*. Conversely, an increase in this ratio causes activation of gene expression by FciA to overcome repression by FciB, leading to high expression of *mpeZ*, *fciC*, and unk10. The activation of *mpeZ* expression increases the proportion of the blue light-absorbing PUB content within phycobilisomes, which increases growth and the efficiency of photon capture (9). FciC and Unk10 are ORFs whose functions have not yet been determined, and their contribution to CA4 is unclear.

In 9916, the regulation of the CA4 response by FciA and FciB resulted in increased gene expression of three genes in blue light (Table S1, Fig. 3, and Fig. S6). This finding suggests that the ancestor of 9916 was a green light specialist, with relatively high PEB content, before horizontal acquisition of a CA4 genomic island. After acquisition, the CA4 genomic island conferred cells with the ability to increase the amount of PUB in blue light, in part because of the FciA- and FciB-controlled increase in MpeZ. This hypothesis raises the issue of whether strains of *Synechococcus* that are blue light specialists, with relatively high PUB content, can become CA4 capable. The recent discovery of two types of CA4 genomic islands, which led to the identification of CA4-A and CA4-B strains (16), provides a possible mechanism for CA4 acquisition by blue light specialists. We propose that whereas CA4-A strains such as 9916 were originally green light specialists and developed CA4 capability by acquiring the CA4-A genomic island, which contains blue light-expressed *mpeZ*, CA4-B strains such as *Synechococcus* RS9915 were originally blue light specialists and gained CA4 capability by acquiring the CA4-B genomic island. *fciA* and *fciB* are both present in the CA4-B genomic island, but *mpeZ* is replaced by *mpeW*, which, unlike *mpeZ*, is more highly expressed in green light (16). The existence of two forms of CA4 also makes it unlikely that CA4 was originally present in all marine *Synechococcus* and has been lost.

CA4 regulation in marine *Synechococcus* is significantly different from the regulation of other types of cyanobacterial chromatic acclimation, which use cyanobacteriochrome photoreceptors that act as histidine kinases to control two component system pathways (11, 24). Cyanobacteriochrome-encoding genes appear to be absent from the 9916 genome, and because the CA4 genomic island does not encode any proteins belonging to any known class of photoreceptors or containing any known chromophore-binding domains, how light color regulates CA4 is unknown.

The only known CA4 regulators, FciA and FciB, belong to the AraC family of transcriptional regulators, a large class of proteins that activate or repress transcription to control a variety of cellular

responses, typically by binding small molecules that alter their DNA-binding activity (21, 25, 26). *fciA* and *fciB* transcript levels are similar in blue and green light (Fig. S1 C and D), and we expect that FciA and FciB levels behave correspondingly. If so, then there must be some form of post-translational regulation of these proteins by light color during CA4. Although it is not clear how light color regulates FciA and FciB activity, it appears that the ratio of FciA to FciB alters the CA4 set point (Fig. 4). We propose that variation in this ratio in different CA4-capable *Synechococcus* isolates may provide a mechanism for creating CA4 phenotypic variation in distinct niches of the world's oceans by generating a range of responses to any single blue–green light ratio.

The restricted nature of the gene regulation by FciA and FciB (Fig. 3D) appears to be quite different from other AraC-class family members. Recent RNA-Seq studies of *araC* mutants in *Escherichia coli* and Salmonella demonstrate that AraC has a much broader regulon than previously known (27), and other AraC family members also control large regulons in a diverse set of bacteria (28, 29). The small and highly specific FciA/FciB regulon is also different from the widespread responses in gene expression that have been observed for other forms of chromatic acclimation (13, 30). The limited number of genes that are regulated by FciA and FciB is likely to facilitate the horizontal transfer of this phenotype by minimizing the interactions with gene products produced in the strain receiving the CA4 island, consistent with the "burden hypothesis" (19, 31). Encoding self-regulatory capacity within the island further improves its transferability, because it is generally difficult to confer regulation on systems that have been acquired through horizontal gene transfer (32). It is also possible that little additional fitness is achieved by expanding CA4 regulation to genes outside of this genomic island and/or there may have been insufficient time since the acquisition of CA4 by 9916 to evolve additional regulatory control of genes in other regions of the genome.

The discovery that the CA4 regulators FciA and FciB and the three genes they control are encoded within a *Synechococcus* CA4 genomic island provides an important addition to our understanding of how light color is used effectively for photosynthesis in marine ecosystems. Light use efficiency is also a major problem in the development of solar-powered microbial energy and chemical production (33). The discovery of a compact genomic island that appears to be readily transferrable and possibly contain both the structural and regulatory elements required to improve light capture may be a valuable tool for expanding the versatility of light use by genetically engineered cyanobacterial strains for in vivo biotechnological applications.

Materials and Methods

Strains and Growth Conditions. Growth conditions were similar to those previously described (9). WT cells were genetically unaltered 9916 cells (34), whereas control cells were WT except for the insertion of a mini-Tn5 transposon from pRL27 (35) within the 5'-half of the RS9916_32112 (GenBank accession no. EAU74248) ORF in the 9916 genome, which encodes an uncharacterized protein. This insertion does not affect CA4 and provides comparable kanamycin resistance to the interruption mutant lines used in this study. Semi-continuous cultures were grown in polycarbonate culture flasks at 22 °C in PCR-S11 media in constant light at an irradiance of 10 µmol photons m^{-2} s^{-1} from fluorescent light bulbs unless noted (Chroma 75 T12; General Electric). Filters (LE716 Mikkel Blue and LE738 Jas Green; LEE Filters) were used to generate blue and green light. When necessary, 50 µg µL−1 kanamycin and/or 10 µg $µL^{-1}$ spectinomycin was added to cultures. A Biotek Synergy-MX spectrofluorometer was used to generate fluorescence excitation spectra, and the Ex495:545 ratios were calculated as previously described (9).

fciA and fciB Complementation/Overexpression. To introduce autonomously replicating plasmids into cells for expression, conjugations between E. coli MC1061 and 9916 were performed as described in the SI Materials and Methods section. Individual colonies were picked from plates and were tested by PCR amplification. All transformed cells were maintained with 10 μg μL^{-1} spectinomycin when grown in liquid culture. A list of strains and plasmids used is provided in Table S2 and a list of PCR amplification primers used is provided in Table S3.

RNA Analyses. RNA blot analyses were performed as previously described (9, 36). Briefly, 100 mL of cells were acclimated to blue or green light for at least 7 d, RNA was purified, and at least 5 μg of RNA was added per lane. Radiolabeled DNA probes were used to probe the blots. Values were normalized as previously described (9, 36). For RNA-Seq, libraries were prepared using an Epicentre (Illumina) ScriptSeq complete bacteria kit, and 50-bp, single-read sequencing was performed using an Illumina HiSeq2000. Fastq reads were trimmed for low quality and adapter sequences using Trimmomatic (version 0.33; default parameters except LEADING:3 TRAILING:3 SLIDINGWINDOW:4:20 MINLEN:50) and stripped of any poly-Gs in sequencing reads. Reads were reference-mapped using Bowtie2 version 2.1.0 (37), and counts for genes and intergenic regions were tabulated using custom Perl scripts and analyzed for differential expression using DESeq (38).

HPLC Separation of Phycobiliproteins. Phycobilisomes were purified as described (9, 39). HPLC was used to separate each phycobiliprotein and liquid chromatography–tandem MS (LC-MS/MS) analyses were performed on fractions collected from a C4 column and digested with trypsin as described previously (9, 40).

UV-VIS Absorption Spectroscopy–MS/MS of Purified Phycobiliproteins. HPLC-separated and trypsin-digested phycobiliproteins from WT, *fciA*, or *fciB* mutant cells grown in blue or green light were analyzed by UV-VIS and MS/MS as described (9). A list of relevant peptide sequences and their characteristics from the *fciA* and *fciB* mutants is provided in Table S4.

ACKNOWLEDGMENTS. We thank Lisa Wiltbank, Jake McKinlay, and Roger Hangarter for helpful discussions. We thank Doug Rusch and James Ford for assistance with RNA-Seq. This research was supported by National Institutes of Health Training Grant T32-GM007757 (to J.E.S.), National Science Foundation Grants MCB-1029414 (to D.M.K.) and MCB-1244339 (to W.M.S.), and by the Office of the Vice Provost for Research at Indiana University, Bloomington, through its Bridge Funding Program (D.M.K.).

REFERENCES

1. Flombaum P, et al. (2013) Present and future global distributions of the marine Cyanobacteria *Prochlorococcus* and *Synechococcus*. Proc Natl Acad Sci USA 110(24):9824–9829.
2. Six C, et al. (2007) Diversity and evolution of phycobilisomes in marine *Synechococcus* spp.: A comparative genomics study. Genome Biol 8(12):R259.
3. Ong LJ, Glazer AN (1991) Phycoerythrins of marine unicellular cyanobacteria. I. Bilin types and locations and energy transfer pathways in *Synechococcus* spp. phycoerythrins. J Biol Chem 266(15):9515–9527.
4. Fairchild CD, et al. (1992) Phycocyanin alpha-subunit phycocyanobilin lyase. Proc Natl Acad Sci USA 89(15):7017–7021.
5. Scheer H, Zhao KH (2008) Biliprotein maturation: The chromophore attachment. Mol Microbiol 68(2):263–276.

6. Ong LJ, Glazer AN, Waterbury JB (1984) An unusual phycoerythrin from a marine cyanobacterium. Science 224(4644):80–83.

7. Palenik B (2001) Chromatic adaptation in marine *Synechococcus* strains. Appl Environ Microbiol 67(2):991–994.

8. Everroad C, et al. (2006) Biochemical bases of type IV chromatic adaptation in marine *Synechococcus* spp. J Bacteriol 188(9):3345–3356.

9. Shukla A, et al. (2012) Phycoerythrin-specific bilin lyase-isomerase controls blue-green chromatic acclimation in marine *Synechococcus*. Proc Natl Acad Sci USA 109(49): 20136–20141.

10. Campbell D (1996) Complementary chromatic adaptation alters photosynthetic strategies in the cyanobacterium *Calothrix*. Microbiology 142(5):1255–1263.

11. Gutu A, Kehoe DM (2012) Emerging perspectives on the mechanisms, regulation, and distribution of light color acclimation in cyanobacteria. Mol Plant 5(1):1–13.

12. Hirose Y, Narikawa R, Katayama M, Ikeuchi M (2010) Cyanobacteriochrome CcaS regulates phycoerythrin accumulation in *Nostoc punctiforme*, a group II chromatic adapter. Proc Natl Acad Sci USA 107(19):8854–8859.

13. Gan F, et al. (2014) Extensive remodeling of a cyanobacterial photosynthetic apparatus in far-red light. Science 345(6202):1312–1317.

14. Dishon G, et al. (2012) Optical habitats of ultraphytoplankton groups in the Gulf of Eilat (Aqaba), Northern Red Sea. Int J Remote Sens 33(9):2683–2705.

15. Stomp M, Huisman J, Stal LJ, Matthijs HCP (2007) Colorful niches of phototrophic microorganisms shaped by vibrations of the water molecule. ISME J 1(4):271–282.

16. Humily F, et al. (2013) A gene island with two possible configurations is involved in chromatic acclimation in marine *Synechococcus*. PLoS One 8(12):e84459.

17. Paz-Yepes J, Brahamsha B, Palenik B (2013) Role of a microcin-C-like biosynthetic gene cluster in allelopathic interactions in marine *Synechococcus*. Proc Natl Acad Sci USA 110(29):12030–12035.

18. Stuart RK, Brahamsha B, Busby K, Palenik B (2013) Genomic island genes in a coastal marine *Synechococcus* strain confer enhanced tolerance to copper and oxidative stress. ISME J 7(6):1139–1149.

19. Wiedenbeck J, Cohan FM (2011) Origins of bacterial diversity through horizontal genetic transfer and adaptation to new ecological niches. FEMS Microbiol Rev 35(5):957–976.

20. Garczarek L, et al. (2008) Function and evolution of the psbA gene family in marine *Synechococcus*: *Synechococcus* sp. WH7803 as a case study. ISME J 2(9):937–953.

21. Schleif R (2010) AraC protein, regulation of the L-arabinose operon in *Escherichia coli*, and the light switch mechanism of AraC action. FEMS Microbiol Rev 34(5):779–796.

22. Humily F, et al. (2014) Development of a targeted metagenomic approach to study a genomic region involved in light harvesting in marine *Synechococcus*. FEMS Microbiol Ecol 88(2):231–249.

23. Wood AM, Phinney DA, Yentsch CS (1998) Water column transparency and the distribution of spectrally distinct forms of phycoerythrin-containing organisms. Mar Ecol Prog Ser 162:25–31.

24. Hirose Y, et al. (2013) Green/red cyanobacteriochromes regulate complementary chromatic acclimation via a protochromic photocycle. Proc Natl Acad Sci USA 110(13):4974–4979.

25. Gallegos MT, Schleif R, Bairoch A, Hofmann K, Ramos JL (1997) Arac/XylS family of transcriptional regulators. Microbiol Mol Biol Rev 61(4):393–410.

26. Tobes R, Ramos JL (2002) AraC-XylS database: A family of positive transcriptional regulators in bacteria. Nucleic Acids Res 30(1):318–321.

27. Stringer AM, et al. (2014) Genome-scale analyses of Escherichia coli and Salmonella enterica AraC reveal noncanonical targets and an expanded core regulon. J Bacteriol 196(3):660–671.

28. Hampel KJ, et al. (2014) Characterization of the GbdR regulon in *Pseudomonas aeruginosa*. J Bacteriol 196(1):7–15.

29. Tan A, et al. (2015) Evolutionary adaptation of an AraC-like regulatory protein in *Citrobacter rodentium* and Escherichia species. Infect Immun 83(4):1384–1395.

30. Stowe-Evans EL, Ford J, Kehoe DM (2004) Genomic DNA microarray analysis: Identification of new genes regulated by light color in the cyanobacterium *Fremyella diplosiphon*. J Bacteriol 186(13):4338–4349.

31. Riedl R (1978) Order in Living Organisms: Systems Analysis of Evolution (Wiley, Chichester, NY), 313 pp.

32. Dorman CJ (2014) H-NS-like nucleoid-associated proteins, mobile genetic elements and horizontal gene transfer in bacteria. Plasmid 75:1–11.

33. Pruvost J, Cornet JF, Le Borgne F, Goetz V, Legrand J (2015) Theoretical investigation of microalgae culture in the light changing conditions of solar photobioreactor production and comparison with cyanobacteria. Algal Res 10:87–99.

34. Fuller NJ, et al. (2003) Clade-specific 16S ribosomal DNA oligonucleotides reveal the predominance of a single marine *Synechococcus* clade throughout a stratified water column in the Red Sea. Appl Environ Microbiol 69(5):2430–2443.

35. McCarren J, Brahamsha B (2005) Transposon mutagenesis in a marine *Synechococcus* strain: Isolation of swimming motility mutants. J Bacteriol 187(13):4457–4462.

36. Seib LO, Kehoe DM (2002) A turquoise mutant genetically separates expression of genes encoding phycoerythrin and its associated linker peptides. J Bacteriol 184(4):962–970.

37. Langmead B, Salzberg SL (2012) Fast gapped-read alignment with Bowtie 2. Nat Methods 9(4):357–359.

38. Love MI, Huber W, Anders S (2014) Moderated estimation of fold change and dispersion for RNA-seq data with DESeq2. Genome Biol 15(12):550.

39. Collier JL, Grossman AR (1992) Chlorosis induced by nutrient deprivation in *Synechococcus* sp. strain PCC 7942: Not all bleaching is the same. J Bacteriol 174(14):4718–4726.

40. Biswas A, et al. (2011) Characterization of the activities of the CpeY, CpeZ, and CpeS bilin lyases in phycoerythrin biosynthesis in *Fremyella diplosiphon* strain UTEX 481. J Biol Chem 286(41):35509–35521.

41. Brahamsha B (1996) A genetic manipulation system for oceanic cyanobacteria of the genus *Synechococcus*. Appl Environ Microbiol 62(5):1747–1751.

42. Elhai J, Wolk CP (1988) Conjugal transfer of DNA to cyanobacteria. Methods Enzymol 167:747–754.

43. Meyer R, Figurski D, Helinski DR (1977) Physical and genetic studies with restriction endonucleases on the broad host-range plasmid RK2. Mol Gen Genet 152(3):129–135.

Legends to Figures

Fig. 1. CA4 genomic island-encoded regulators FciA and FciB inversely control chromatic acclimation. (A) Genomic context and GC ratio of the 9916 CA4 genomic island. Blue and black lines indicate the average GC ratio inside the genomic island and in flanking regions that are more representative of the overall genome. (B) Color phenotypes of 9916 WT (Left), *fciA*− mutant (Center), and fciB− mutant (Right) cultures after growth in blue or green light. (C) Ex495:545 fluorescence excitation ratio, with the emission set at 580 nm, from control (black circles), *fciA*− mutant (red squares), and *fciB*− mutant (orange triangles) cells. Semi-continuously diluted cultures were allowed to acclimate to green light, shifted to blue light on day 3, and shifted back to green light on day 18. Error bars are the SEM of three independent replicates. (D) Complementation and overexpression analyses of *fciA* and *fciB* in WT (Left), *fciA*− (Center), and *fciB*− mutant (Right) cells. For each of the three genotypes, the negative control cells possess the plasmid without an insert (empty), whereas the plasmid-expressed gene(s) is indicated by a plus symbol. Steady-state Ex495:545 ratios are for cells acclimated to blue light (blue bars) or green light (green bars) for at least 7 d; error bars are the SEM of three independent replicates.

Fig. 2. FciA and FciB control all chromophorylation changes in 9916 during CA4. A schematic representation of the predominant chromophore composition in 9916 phycobilisomes for each condition and genetic background is shown above each set of samples. (Upper) Red phycobilisomes indicate higher PEB levels and orange phycobilisomes indicate higher PUB levels. (Lower) Absorption spectra of HPLC-purified CpeA (A–C) or MpeA (D–F) from WT, *fciA*, or *fciB* mutant cells, indicated above, and grown in blue (blue line) or green (green line) light. PUB absorbance is at 494 nm, and PEB absorbance is at 552 nm. Spectra shown are representative of at least three independent isolations and analyses from each cell type and light color. Note that amplitudes of absorbance values of independent spectra cannot be compared quantitatively. Only the presence/absence of any particular absorbance and the relative ratios of absorbances within a spectrum can be quantitatively compared with another spectrum. The amplitudes of the absorbance values for blue light- and green light-grown samples for each mutant and protein type therefore have been slightly offset for ease of comparison.

Fig. 3. FciA and FciB inversely regulate transcript levels of three genes within the 9916 CA4 genomic island. Mean RNA-Seq transcript levels for *mpeZ* (A), *fciC* (B), and *unk10* (C) in 9916 cells. Control, *fciA*−, and *fciB*− mutant cell cultures were acclimated to blue light (BL) or green light (GL) for at least 7 d before RNA extraction. Mean expression value of RNA from control cells grown in blue light was set to 100%. Relative expression is based on normalized read counts. Error bars are the SEM from three independent replicates. (D) Venn diagram of the 9916 genes shown by RNASeq to be regulated by blue and green light, FciA, and FciB. The three genes regulated by blue and green light, FciA, and FciB are in red.

Fig. 4. Overexpression of *fciA* or *fciB* shifts the CA4 midpoint value in 9916. Steady-state Ex495:545 ratios were measured for transformed cells grown in various ratios of blue (BL) and green (GL) light, with a constant total irradiance of 10 µmol photons m^{-2} s^{-1}. WT cells carrying either the empty vector (circles), *fciA* only (squares), *fciB* only (upward triangles), or *fciA* and *fciB* together (downward triangles) were grown in the blue:green light ratios shown along the x axis for at least 7 d, and then Ex495:545 ratios were measured. Error bars are the SEM of three independent replicates.

Fig. 5. Widespread distribution and model for CA4 regulation. (A) Distribution of Synechococcus strains currently known to be capable of CA4. The strain used in this study, 9916, is denoted with an

orange star. (B) Preliminary model of CA4 regulation. FciB represses the expression of *mpeZ*, *fciC*, and *unk10* when green light predominates, which leads to phycobilisomes that are more red and contain more PEB. When blue light is more prevalent, FciA activates expression of *mpeZ*, *fciC*, and *unk10*, leading to phycobilisomes that are more orange and contain more PUB. MpeZ, the only CA4-regulated gene whose function is known, is more highly expressed in blue light. MpeZ converts PEB into PUB and attaches it to MpeA-C83.

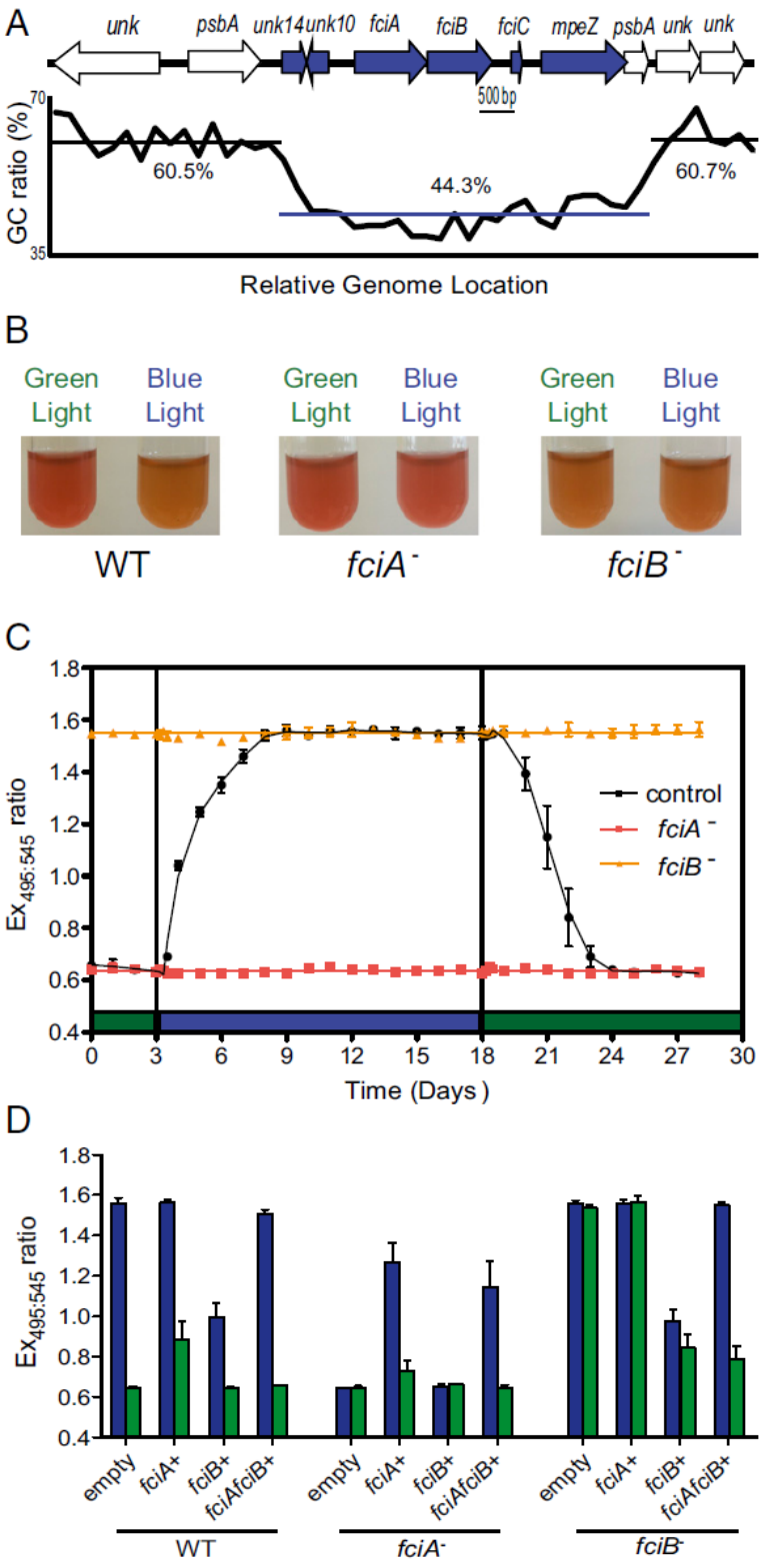

Sanfilippo et al. Fig. 1

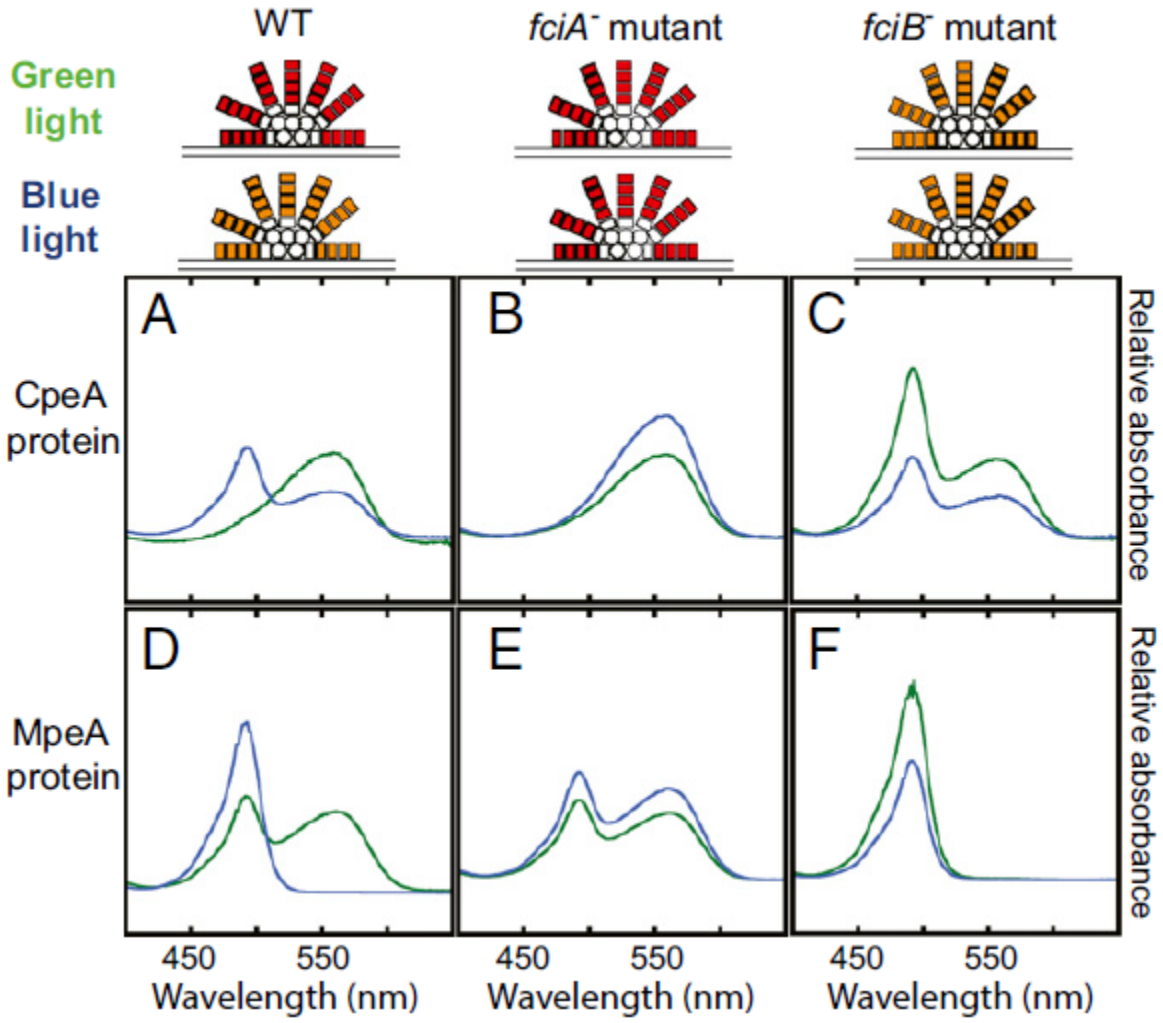

Sanfilippo et al. Fig. 2

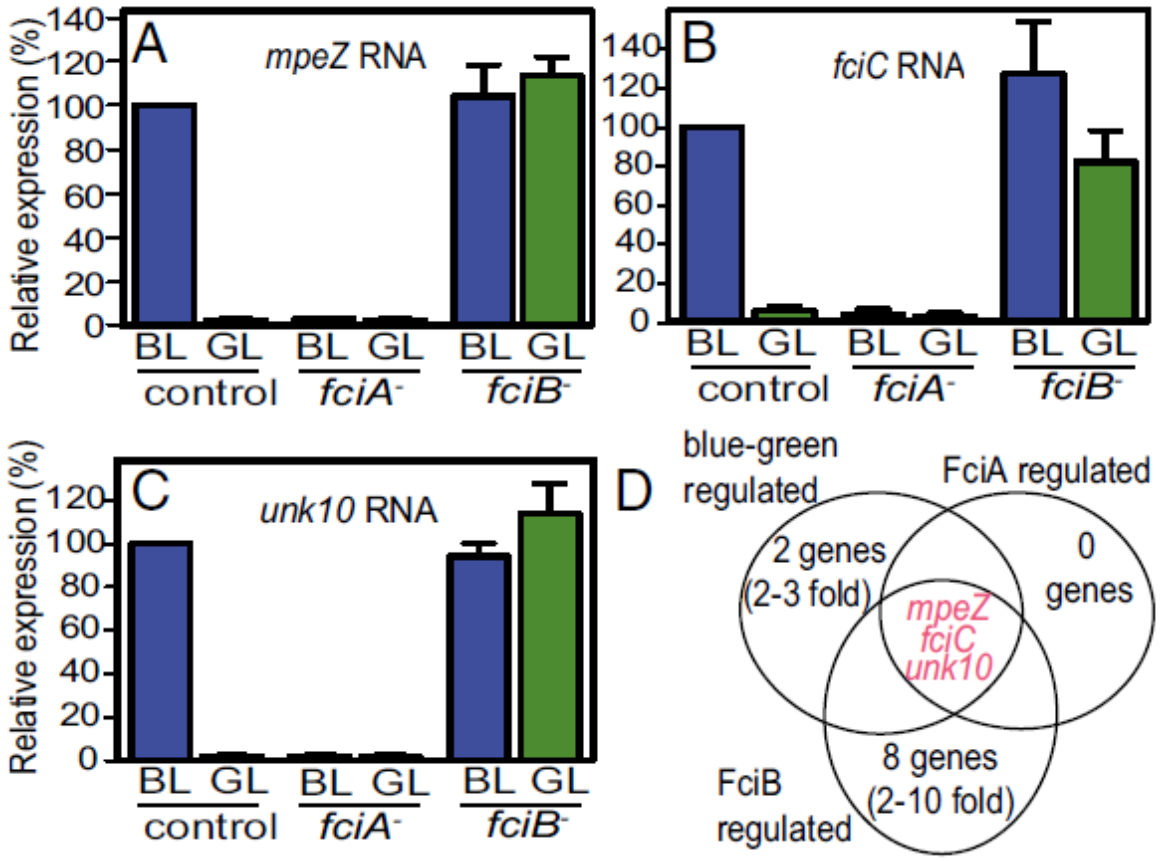

Sanfilippo et al. Fig. 3

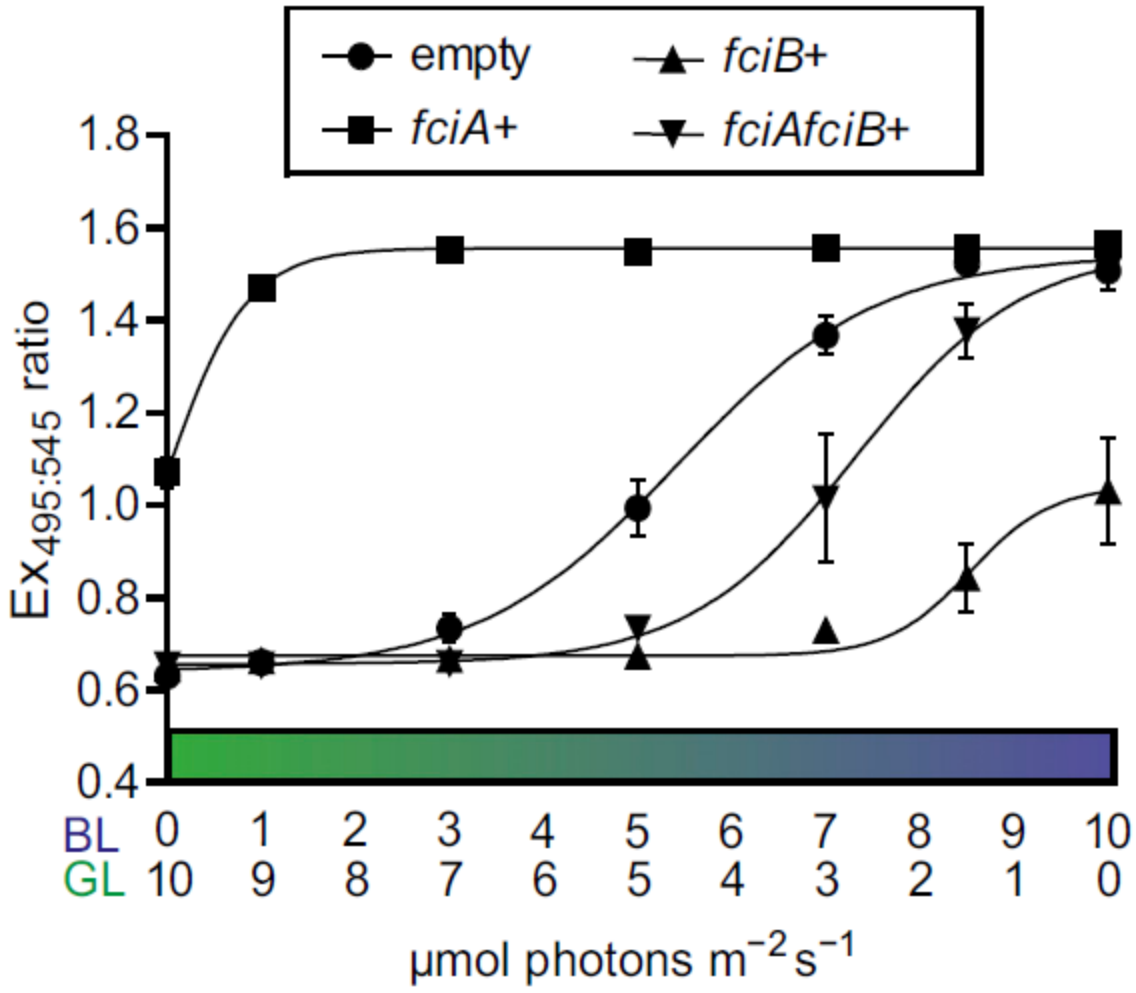

Sanfilippo et al. Fig. 4

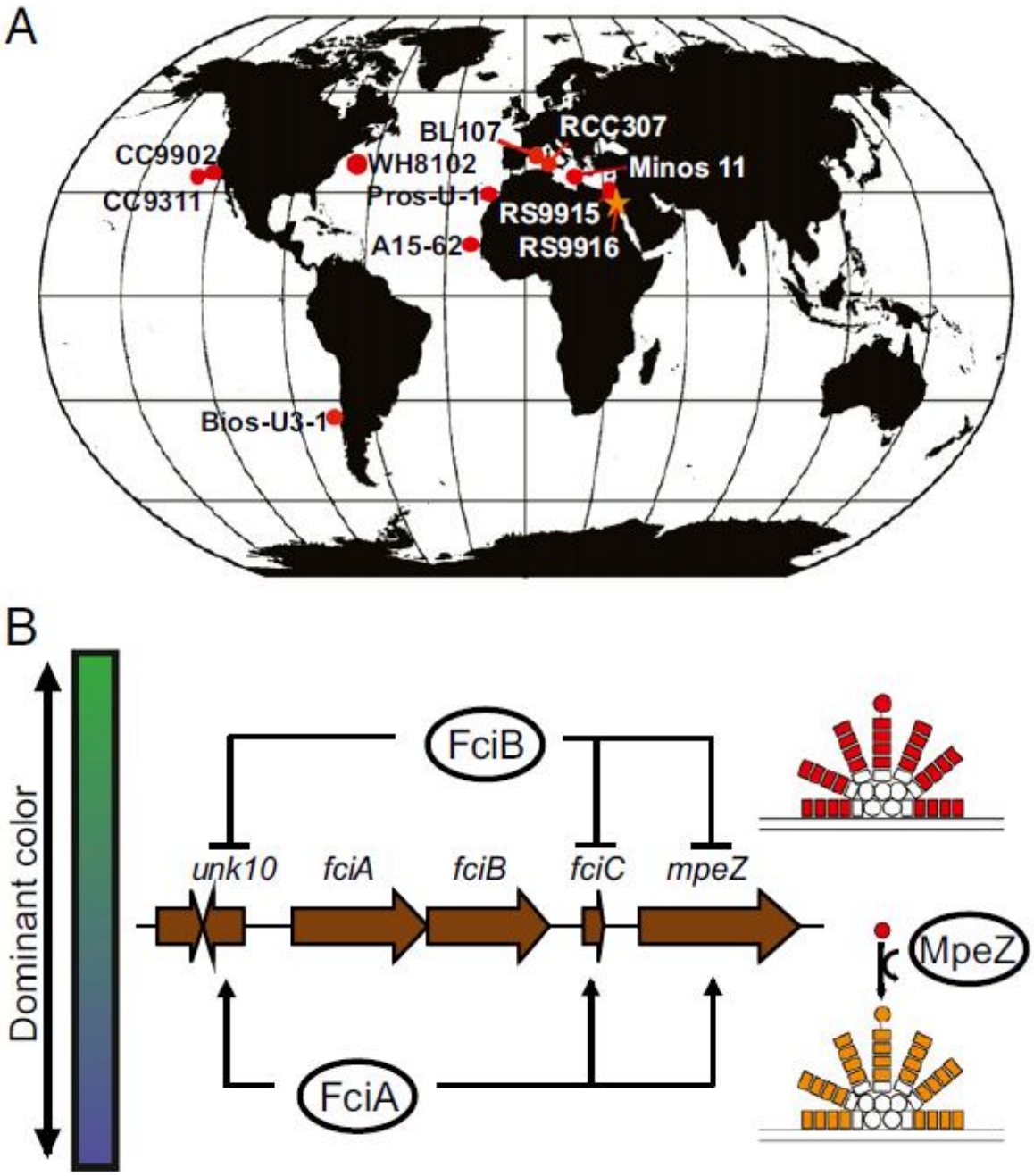

Sanfilippo et al. Fig. 5

Supporting Information

SI Materials and Methods

Plasmid Construction. The plasmids and primers used are listed in Tables S2 and S3. pASfciA and pASfciB were made by PCR amplification of ~800-nt internal regions of *fciA* and *fciB* and cloning into the BamHI site of pMUT100. pJS2 and pJS3 were made by PCR amplification of the promoter and ribosomebinding site of *fciA* and either *fciA* or *fciA* and *fciB*, which were cloned into the BamHI and EagI sites of pJS1. pJS4 was generated by PCR amplification and fusion of the promoter and ribosome-binding site of *fciA* to the *fciB* gene. The translational fusion was then cloned into the BamHI and EagI sites of pJS1.

***fciA* and *fciB* Disruption**. Gene disruptions were generated as previously described (9, 41). Briefly, *E. coli* MC1061, a conjugative strain containing pRK24 and PRL528, was transformed with plasmids designed for disruption. Conjugations were performed with the conjugative strain and 9916 cells, which were then plated in 0.3% agar plates containing 50 μg μL^{-1} kanamycin. Individual colonies were picked from plates and tested for the proper insertion by PCR amplification of the regions and DNA sequencing. All transformed cells were maintained with 50 μg μL^{-1} kanamycin when grown in liquid culture.

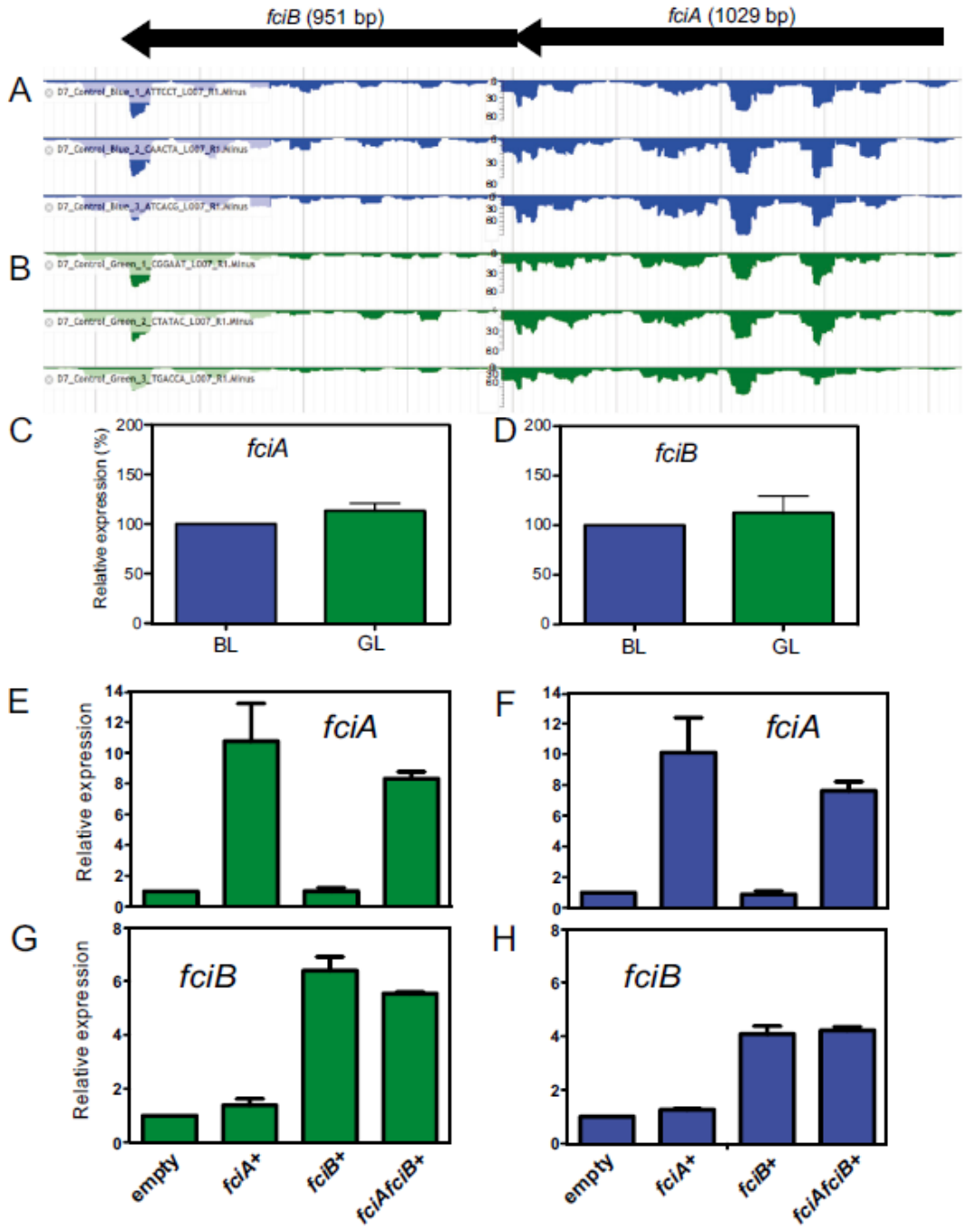

Fig. S1. *fciA* and *fciB* RNA abundance measurements in control cells and in transformed lines overexpressing *fciA*, fciB, or both together. RNA-Seq data indicate that *fciA* and *fciB* are cotranscribed and not CA4-regulated in 9916. (A and B) Raw RNA-Seq results for three independent biological replicates of control cells grown in blue light (BL) (A) and green light (GL) (B). Only the RNAs encoded by the *fciAB* template strand are shown; the y axis for each result is the total number of reads obtained. Relative mean transcript levels after DESeq2 normalization (38) in blue light and green light for fci*A* (C) and fciB (D), with the blue light expression levels set to 100%. Error bars are the SEM for three independent biological replicates. RNA blot analyses were used to measure mean transcript levels of *fciA* (E and F) or *fciB* (G and H) in WT 9916 cells transformed with either an empty plasmid vector (empty) or a plasmid containing *fciA* (*fciA*+), *fciB* (*fciB*+), or both *fciA* and *fciB* (*fciAfciB+*) and grown in either green (E and G) or blue (F and H) light. Values from cells containing the empty vector,

after ribosomal RNA normalization, were set to 1. Error bars are the SEM from three independent replicates.

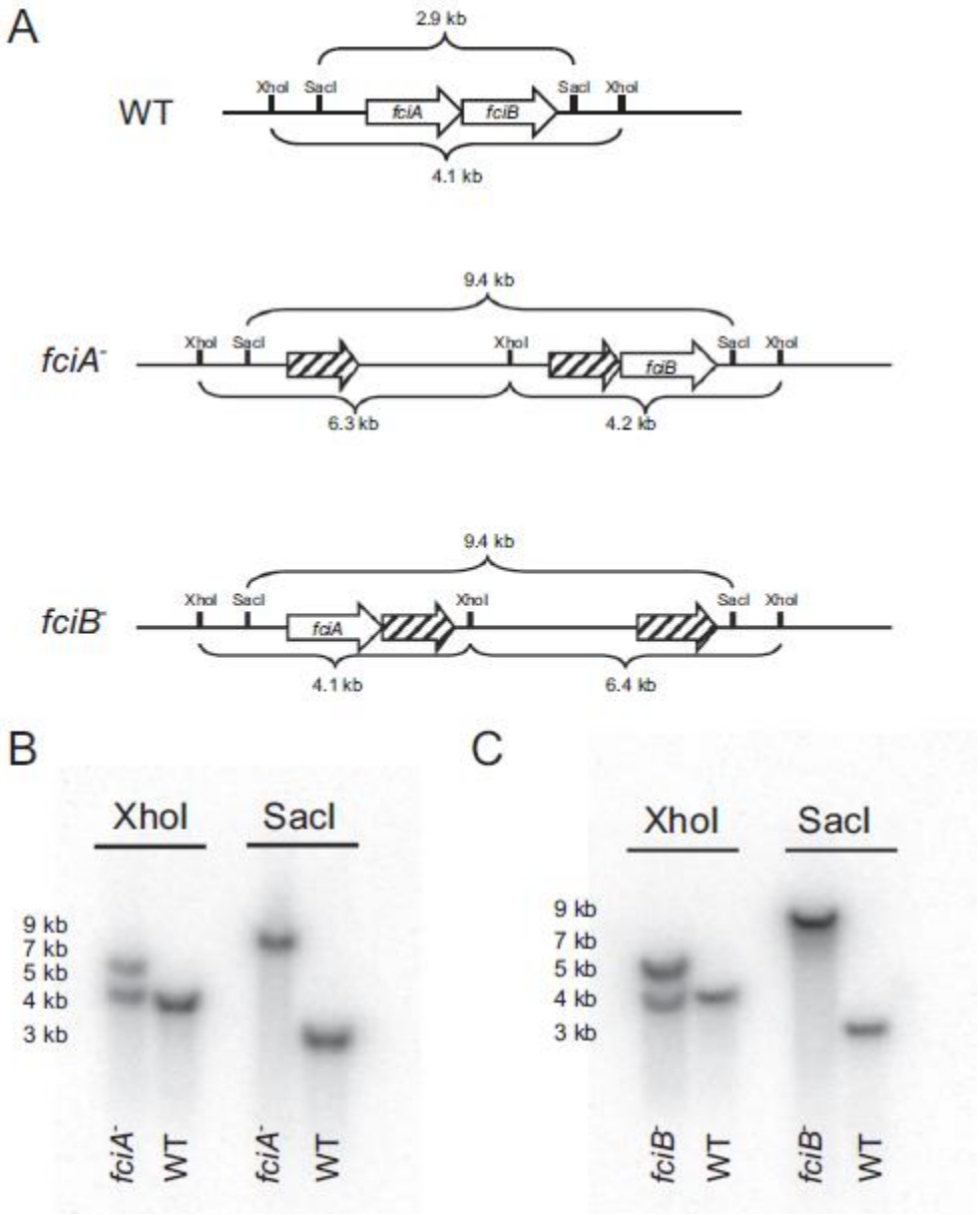

Fig S2. Southern blot analysis of interruption of *fciA* and *fciB* in 9916. (A) Schematic diagram of the region of the 9916 genome containing *fciA* and *fciB*, showing the interruptions of these genes in the insertion mutants generated for this study and the restriction enzyme cutting patterns predicted for the WT, *fciA*−, and *fciB*− mutants. (B and C) Phosphorimages of the radioactive blots obtained for the *fciA* mutant (B) and the fciB mutant (C), each analyzed with WT, after cutting of DNA with the restriction enzymes indicated. Blots were probed with a radiolabeled double-stranded DNA fragment from either *fciA* (B) or *fciB* (C).

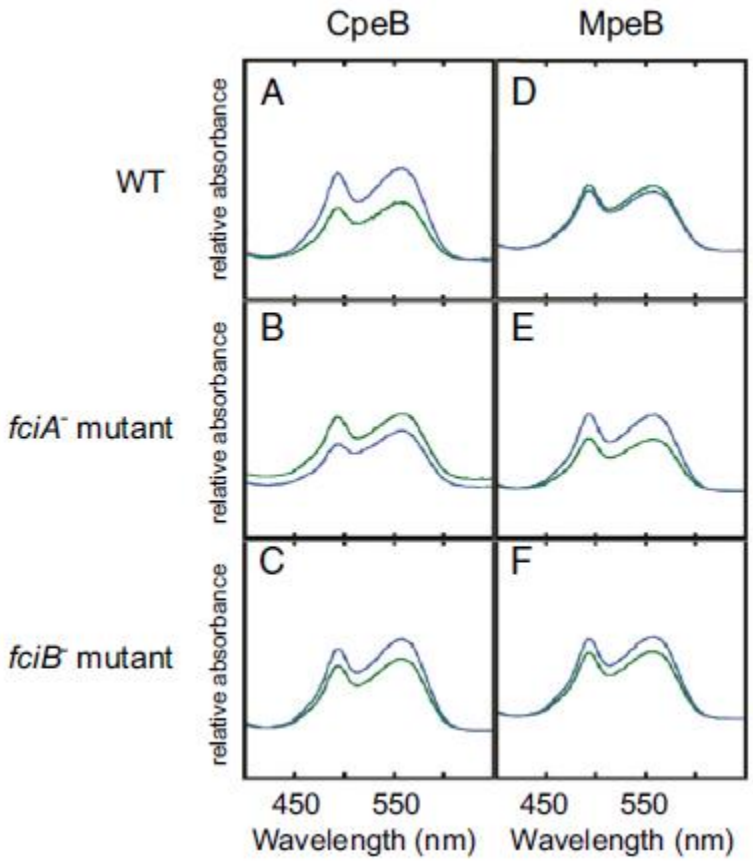

Fig. S3. FciA and FciB do not affect the chromophorylation of CpeB or MpeB in blue or green light. Visible absorption spectra of HPLC-purified CpeB from WT (A), *fciA*− (B), or *fciB*− (C) cells grown in blue light (blue line) or green light (green line) and of HPLC-purified MpeB from WT (D), *fciA*− (E), or *fciB*− (F) cells grown in blue light (blue line) or green light (green line). PUB absorbance is at 490 nm, and PEB absorbance is at 552 nm. Spectra shown are representative of at least three independent isolations and analyses from each cell and protein type in each light color. Note that amplitudes of absorbance values of independent spectra cannot be compared quantitatively. Only the presence/absence of any particular absorbance and the relative ratios of absorbances within a spectrum can be quantitatively compared with another spectrum. The amplitudes of the absorbance values for blue light- and green light-grown samples for each mutant and protein type therefore have been slightly offset for ease of comparison.

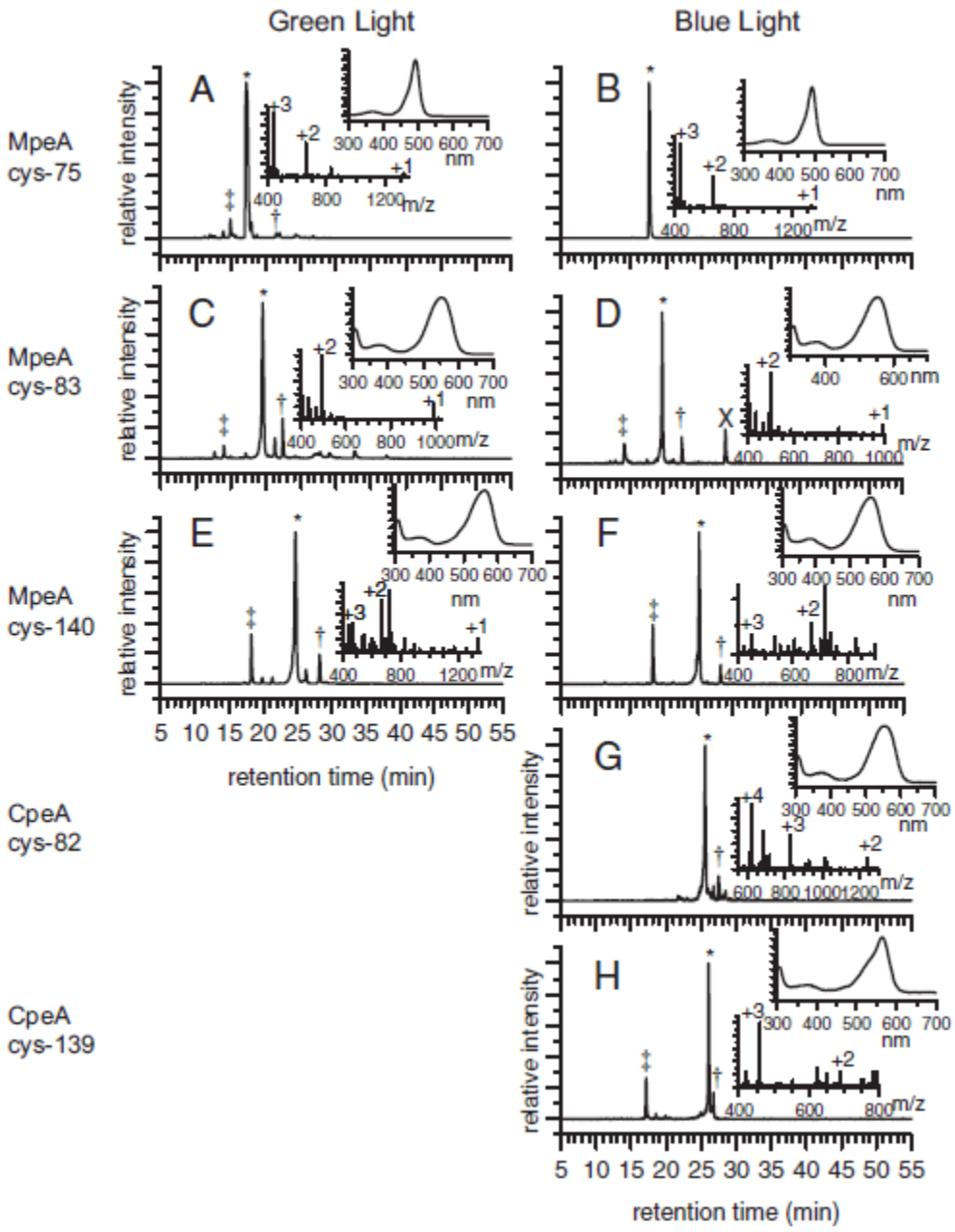

Fig. S4. LC-VIS-MS analyses of the chromophores attached to the MpeA (A–F) and CpeA (G–H) subunits of the phycobilisomes in the fciA mutant after growth in green (A, C, and E) or blue (B, D, and F–H) light; * indicates the major extracted-ion chromatogram peak for which the MS and UV-VIS spectra are shown; † indicates a minor extracted-ion chromatogram peak for which an absorbance max at 490 nm (suggesting PUB attachment) was observed along with peptide ions, consistent with the sequence indicated in Table S4. ‡ indicates a minor extracted-ion chromatogram peak that contained mass spectral features consistent with ions 2 Da lighter than predicted for the sequence in found in Table S4, with a visible spectrum slightly red shifted from that of PEB. X indicates an ion with a similar m/z to a bilin-containing peptide but has the wrong charge and/or lacks a corresponding visible absorbance band. The numbers in each mass spectrum indicate the charge state of the ion. Peptide sequence information is provided in Table S4.

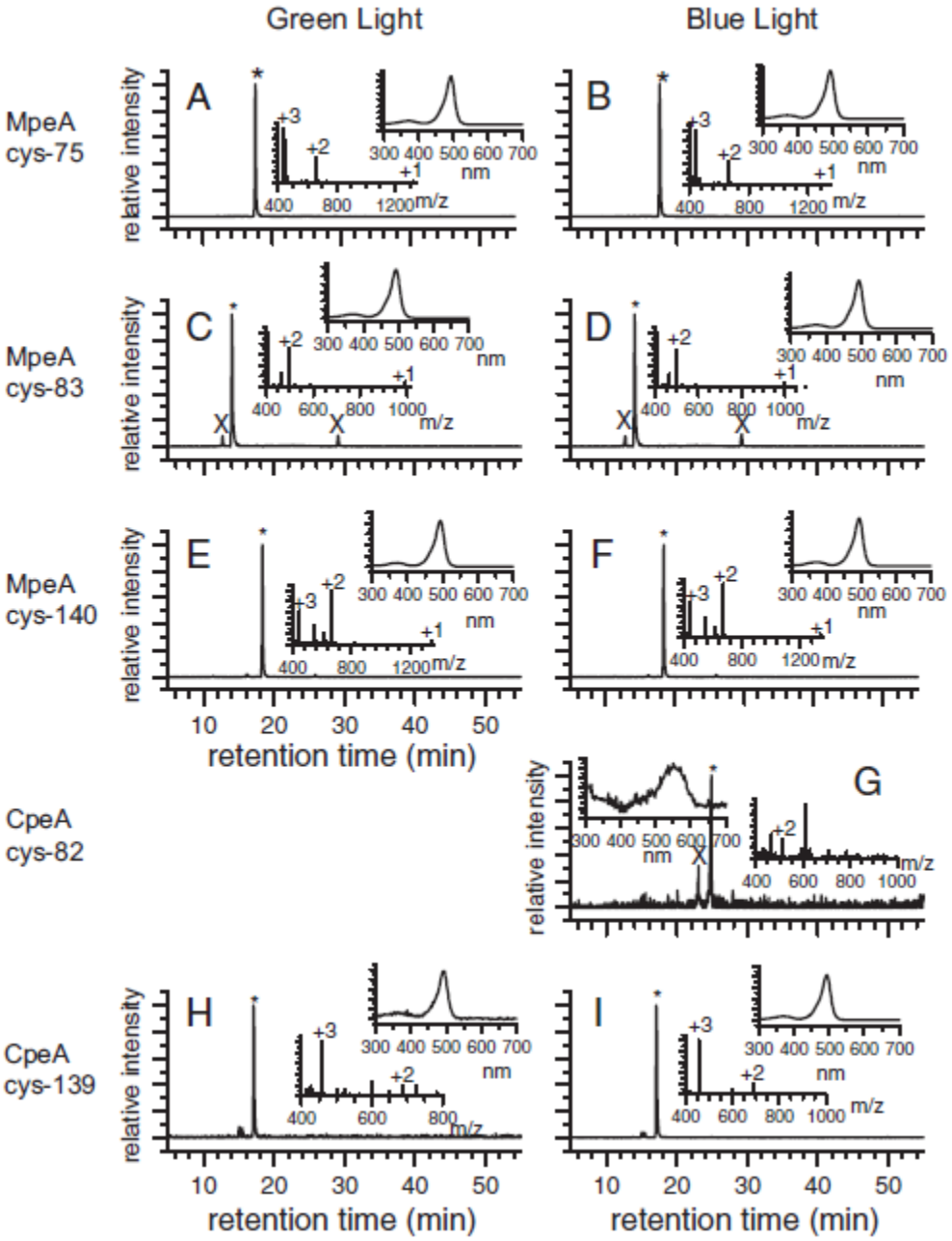

Fig. S5. LC-VIS-MS analyses of the chromophores attached to the MpeA (A–F) and CpeA (G–I) subunits of the phycobilisomes in the fciB mutant after growthin green (A, C, E, and H) or blue (B, D, F, G, and I) light; * indicates the major extracted-ion chromatogram peak for which the MS and UV-VIS spectra are shown. The numbers in each mass spectrum indicate the charge state of the ion. X indicates an ion with a similar m/z to a bilin-containing peptide but has the wrongcharge and/or lacks a corresponding visible absorbance band. Peptide sequence information is provided in Table S4.

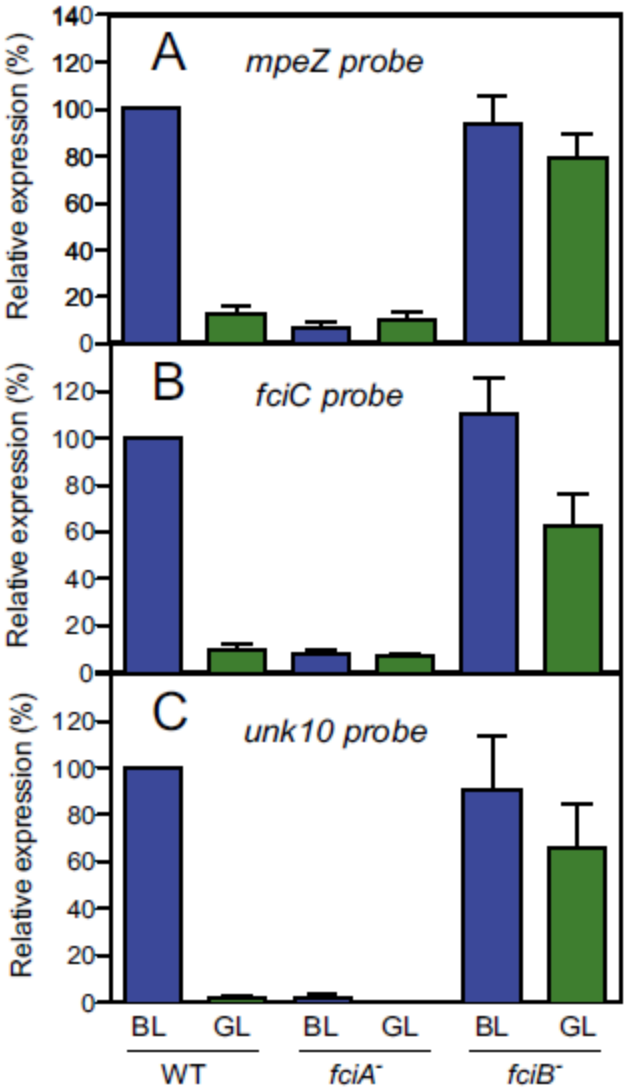

Fig. S6. RNA blot verification of RNA-Seq data. Mean transcript levels for *mpeZ* (A), *fciC* (B), and *unk10* (C) in WT, *fciA*−, and *fciB*− mutant cells acclimated toblue light (BL) or green light (GL) for at least 7 d. Values from blue light-grown WT cells after ribosomal normalization were set to 100%. Error bars are the SEM from six independent replicates.

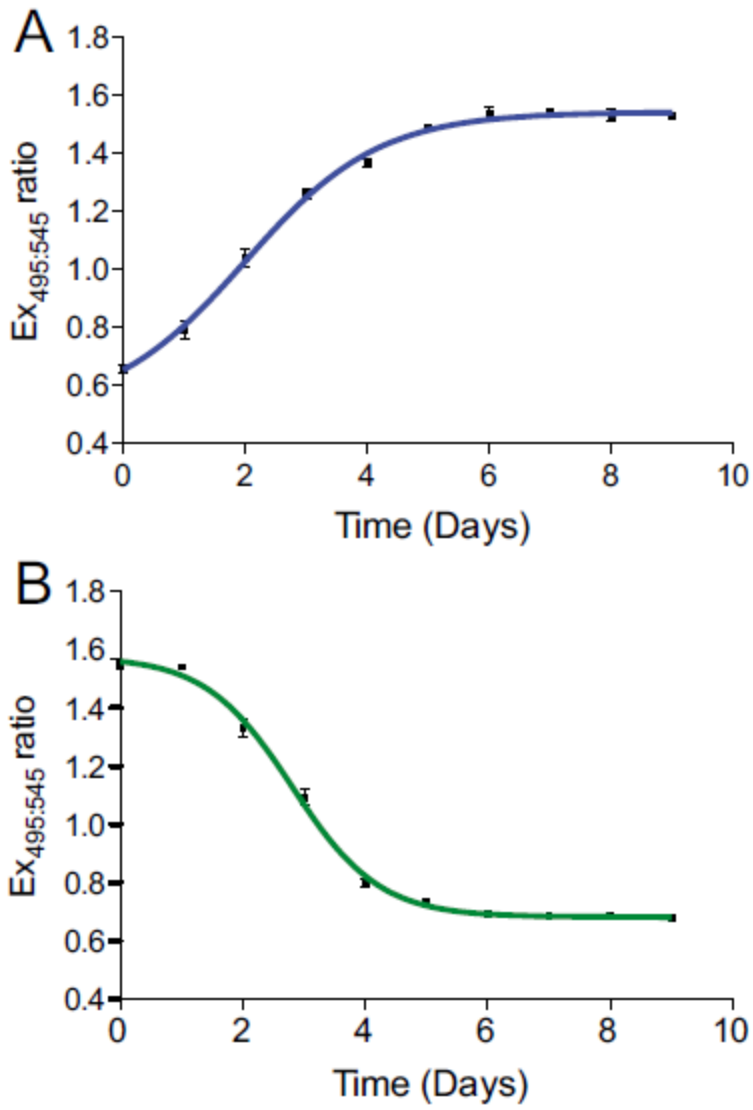

Fig. S7. Low blue or green light irradiances are sufficient to trigger the conversion from one CA4 state to the other.WT cells containing the empty vector pJS1 were grown in 3 µmol photons m^{-2} s^{-1} of light throughout the experiment. On day 0, experimental cells were switched from green light to blue light (A) and blue light to green light (B), and Ex495:545 ratios were measured and calculated daily. Error bars are the SEM from three independent replicates.

Table S1. RNA-Seq data for control, *fciA*, and *fciB* mutants

Genes	Locus tag	GenBank accession no.	Fold change	Adjusted *P*
Control blue light vs. control green light				
Genes higher in blue light				
unk10	RS9916_39551	EAU72764.1	40.1	$7.57 \times e^{-34}$
mpeZ	RS9916_39531	EAU72760.1	35.3	$1.53 \times e^{-22}$
fciC	RS9916_39536	EAU72761.1	9.8	0.0001
Membrane protein	RS9916_26829	EAU73195.1	2.5	0.0065
RNA polymerase sigma factor, type II	RS9916_38072	EAU75440.1	2.1	0.0393
Genes higher in green light				
None	—	—	—	—
fciA mutant blue light vs. control blue light				
Genes lower in *fciA* mutant				
unk10	RS9916_39551	EAU72764.1	38.7	$5.50 \times e^{-33}$
mpeZ	RS9916_39531	EAU72760.1	27.1	$3.91 \times e^{-19}$
fciC	RS9916_39536	EAU72761.1	12.9	$1.07 \times e^{-5}$
Genes lower in control				
None	—	—	—	—
fciB mutant green light vs. control green light				
Genes higher in *fciB* mutant				
unk10	RS9916_39551	EAU72764.1	44.1	$1.21 \times e^{-35}$
mpeZ	RS9916_39531	EAU72760.1	38.5	$1.16 \times e^{-23}$
Pirin-related protein	RS9916_36727	EAU75171.1	10.3	$7.86 \times e^{-17}$
fciC	RS9916_39536	EAU72761.1	8.6	0.0003
NADPH-dependent FMN reductase	RS9916_36722	EAU75170.1	8.4	$1.18 \times e^{-6}$
Rubrerythrin	RS9916_36712	EAU75168.1	6.9	$3.50 \times e^{-8}$
Type IV pilin PilA	RS9916_32652	EAU74356.1	5.0	0.0192
ABC-type sugar transporter, permease component	RS9916_31622	EAU74150.1	2.8	0.0120
2-Cys peroxiredoxin	RS9916_30189	EAU73865.1	2.6	0.0189
Genes higher in control				
Small heat shock protein (HSP20) family protein	RS9916_36677	EAU75161.1	3.4	0.0021
ATP-dependent Clp protease, ATP-binding subunit	RS9916_27694	EAU73368.1	2.1	0.0120

Dashes indicate not applicable.

Table S2. List of strains and plasmids used

Strain or plasmid	Description
Strain	
WT	*Synechococcus* RS9916, isolated from the Red Sea (34)
Control	Kan^R, mini-Tn5 insertion in uncharacterized gene RS9916_32112
fciA$^-$	Kan^R, plasmid insertion disrupting *fciA*
fciB$^-$	Kan^R, plasmid insertion disrupting *fciB*
WT pJS1	$Spec^R$, contains autonomously replicating empty vector
WT pJS2	$Spec^R$, contains vector expressing *fciA*
WT pJS3	$Spec^R$, contains vector expressing *fciA* and *fciB*
WT pJS4	$Spec^R$, contains vector expressing *fciB*
fciA$^-$ pJS1	Kan^R $Spec^R$, contains autonomously replicating empty vector
fciA$^-$ pJS2	Kan^R $Spec^R$, contains vector expressing *fciA*
fciA$^-$ pJS3	Kan^R $Spec^R$, contains vector expressing *fciA* and *fciB*
fciA$^-$ pJS4	Kan^R $Spec^R$, contains vector expressing *fciB*
fciB$^-$ pJS1	Kan^R $Spec^R$, contains autonomously replicating empty vector
fciB$^-$ pJS2	Kan^R $Spec^R$, contains vector expressing *fciA*
fciB$^-$ pJS3	Kan^R $Spec^R$, contains vector expressing *fciA* and *fciB*
fciB$^-$ pJS4	Kan^R $Spec^R$, contains vector expressing *fciB*
Plasmid	
pMUT100	Kan^R Suicide vector backbone used for homologous recombination (41)
pRL27	Kan^R Contains mini-Tn5 transposon (35)
pRL528	Helper plasmid, carries *mob* (42)
pRK24	Conjugal plasmid, RK2 derivative (43)
pASfciA	pMUT100 derivative, for disruption of *fciA*
pASfciB	pMUT100 derivative, for disruption of *fciB*
pJS1	$Spec^R$ Derivative of pRL153, autonomously replicating in RS9916 (41)
pJS2	From pJS1, for expression of *fciA*
pJS3	From pJS1, for expression of *fciA* and *fciB*
pJS4	From pJS1, for expression of *fciB*

Kan^R, denotes kanamycin resistance; $Spec^R$, denotes spectinomycin resistance.

Table S3. List of PCR amplification primers used

Primer	Sequence (5′ to 3′)
Mut-BamHI-fciA-for	ATAGGATCCATTGGGCATGGAGGAGTACTGCAA
Mut-BamHI-fciA-rev	ATAGGATCCGCCGTAATACAGGGCATTCTGCTT
Mut-BamHI-fciB-for	ATAGGATCCGCTGAGTTAGGTCAGCAGACAAGA
Mut-BamHI-fciB-rev	ATAGGATCCCGCGAAACGACCTGCATGCTTAAA
mpeZ-probe-for	TTTTGGGCTGCACCGATACT
mpeZ-probe-rev	ACGATGGCTCAGATTTCGCT
fciA-probe-for	TGACAAGCTCGATTTGTGCG
fciA-probe-rev	CAAAGGGGGTAATCCCGGAC
fciB-probe-for	TATGAAGGCTGGGGTACGGA
fciB-probe-rev	TTGGCTAGCGCCTAAATGCT
fciC-probe-for	GGGTGACCTTTGAGCTTAGTGA
fciC-probe-rev	ACTCGCTTATCGATTATCTCAATCA
unk10-probe-for	TCAAAATCCGAATTGCATGCGT
unk10-probe-rev	GCTCCTGATCTAAAATCGCCCT
Exp-BamHI-fciA-for	ACTGGATCCCTGAATTAAAGCCTCTGCCTCTTCTACCG
Exp-EagI-fciA-rev	ACTCGGCCGTTATCTATACCGCATAAGATCAGAAACCAAAACCG
Exp-FciB-fusion1	AGAGTTTTATCATGCTGATGTTCGCTGAAAGTGTGG
Exp-FciB-fusion2	GCGAACATCAGCATGATAAAACTCTCTCTCTCTTATAAAGATCCCCTTC
Exp-EagI-fciB-rev	ACTCGGCCGCTACGAGGCTTGGATAGTTTGACTGGG

for, forward; rev, reverse.

Table S4. Peptide sequences and characteristics from *fciA* and *fciB* mutants

Graph	Light color	Protein	Peptide sequence	Retention time, min	Ion A, m/z	Ion B, m/z	Ion C, m/z	VIS Pk, nm
fciA mutant peptides								
A	Green	MpeA	KC*$_{75}$ATEGK	17.19	441.551^{3+}	661.820^{2+}	1,322.634^{1+}	490
B	Blue	MpeA	KC*$_{75}$ATEGK	17.57	441.545^{3+}	661.818^{2+}	1,322.653^{1+}	490
C	Green	MpeA	C*$_{83}$KR	19.54	496.752^{2+}	992.500^{1+}	NA	550
D	Blue	MpeA	C*$_{83}$KR	19.79	496.749^{2+}	992.508^{1+}	NA	550
E	Green	MpeA	NDGC*$_{140}$SPR	24.67	667.771^{2+}	445.528^{3+}	1,334.568^{1+}	550
F	Blue	MpeA	NDGC*$_{140}$SPR	25.14	667.787^{2+}	445.525^{3+}	1,334.581^{1+}	550
G	Blue	CpeA	QPGEAGSQIKVDKC*$_{82}$YR	25.54	620.789^{4+}	827.387^{3+}	1,240.584^{2+}	550
H	Blue	CpeA	DRAC*$_{139}$APR	26.04	458.884^{3+}	687.827^{2+}	1,374.677^{1+}	550
fciB mutant peptides								
A	Green	MpeA	KC*$_{75}$ATEGK	17.54	441.542^{3+}	661.817^{2+}	1,322.637^{1+}	490
B	Blue	MpeA	KC*$_{75}$ATEGK	17.54	441.542^{3+}	661.817^{2+}	1,322.637^{1+}	490
C	Green	MpeA	C*$_{83}$KR	13.99	496.748^{2+}	992.505^{1+}	NA	490
D	Blue	MpeA	C*$_{83}$KR	13.99	496.747^{2+}	992.503^{+}	NA	490
E	Green	MpeA	NDGC*$_{140}$SPR	18.34	667.785^{2+}	445.523^{3+}	1,334.577^{1+}	490
F	Blue	MpeA	NDGC*$_{140}$SPR	18.34	667.786^{2+}	445.526^{3+}	1,334.588^{1+}	490
G	Blue	CpeA	C*$_{82}$YR	24.87	514.238^{2+}	NA	NA	550
H	Green	CpeA	DRAC*$_{139}$APR	17.09	458.884^{3+}	687.828^{2+}	NA	490
I	Blue	CpeA	DRAC*$_{139}$APR	17.09	458.883^{3+}	687.833^{2+}	1,374.110^{1+}	490

NA, not applicable.